Measurement report: Biogenic VOC emissions profiles of Rapeseed leaf litter and their SOA formation potential

Letizia Abis[1] *, Carmen Kalalian[1], Bastien Lunardelli[1], Tao Wang[2], Liwu Zhang[2], Jianmin Chen[2], Sébastien Perrier[1], Benjamin Loubet[3], Raluca Ciuraru [3] and Christian George[1]

[1] Univ Lyon, Université Claude Bernard Lyon 1, CNRS, IRCELYON, F-69626, Villeurbanne, France.
[2]Shanghai Key Laboratory of Atmospheric Particle Pollution and Prevention, Department of Environmental Science & Engineering, Fudan University, Shanghai,200433, Peoples' Republic of China.
[3]INRAE, UMR ECOSYS, AgroParisTech, Université Paris-Saclay, 78850, Thiverval-Grignon, France
*Now working at: Technische Universität Berlin, Umweltchemie und Luftrinhaltunz, Straße des 17. Juni 135, Berlin, 10623, Germany.

Correspondence to: Christian George (christian.george@ircelyon.univ-lyon1.fr)

Abstract. We analysed the biogenic volatile organic compounds (BVOC) emissions from rapeseed leaves litter and their potential to create secondary organic aerosols (SOA) under three different conditions i.e., (i) in presence of UV light irradiation; (ii) in presence of ozone, and (iii) with both ozone and UV light. These experiments have been performed in a controlled atmospheric simulation chamber containing leaves litter samples, where BVOC and aerosol number concentrations have been measured for 6 days. Our results show that BVOC emission profiles were affected by UV light irradiation, which increased the summed BVOC emissions compared to the experiment with solely O_3. Furthermore, the diversity of emitted VOCs from the rapeseed litter increased also in presence of UV light irradiation. SOA formation was observed when leaves litter were exposed to both UV light and O_3, indicating a potentially large contribution to particle formation or growth at local scales. To our knowledge, this study investigates for the first time the effect of UV irradiation and O_3 exposure on both VOC emissions and SOA formation for leaves litter samples. A detailed discussion about the processes behind the biological production of the most important VOC is proposed.

1 Introduction

Nowadays, the crucial role played by Volatile Organic Compounds (VOCs) as precursors of ozone and particles within the troposphere has been clearly established (Hatfield and Huff Hartz, 2011). Sources of VOCs are either anthropogenic, related to human activities, or biogenic. Biogenic volatile organic compounds (BVOCs) are released from living and senescent vegetation, soils and microorganisms, or oceans (Kesselmeier and Staudt, 1999; Murphy et al., 2010). Such biogenic VOCs (BVOCs) have been estimated to contribute up to 90% of the total VOC emissions (Guenther, 1995). Furthermore, the currently most accredited emission model for BVOC (MEGAN v2.1), estimates that 760 Tg C yr-1 are emitted into troposphere (Sindelarova et al., 2014). Modelling studies highlighted the impact of BVOCs on carbon monoxide (CO), hydroxyl radical (OH), low-level ozone, and thus, the oxidative capacity of the troposphere (Granier et al., 2000; Pfister et al., 2008; Poisson et al., 2000). It is found that products resulting from the BVOC oxidation are significant precursors of Secondary Organic Aerosols (SOA), affecting the Earth's radiative balance (Ziemann and Atkinson, 2012) and thus, the climate and the human health (De Gouw and Jimenez, 2009). In addition, between 11% and 70% of emitted BVOCs are converted into SOA, leading to a yearly production of 140-190 Tg C yr-1 of particles (Hallquist et al., 2009).

Due to the growing awareness about climate change and atmospheric pollution, the number of studies focusing on BVOCs has grown almost exponentially over the past 20 years, with a strong focus on forests and plants since they are their most important sources. However, little attention has been drawn to leaves litter and their contribution to SOA formation in global BVOC emissions model, even if several studies reported a significant contribution to BVOC emissions, and described BVOCs emitted from leaves litter as potential contributors to SOA formation (Bigg, 2004; Faiola et al., 2014; Isidorov and Jdanova, 2002; Viros et al., 2020). The annual global leaves litter production has been estimated between 75 and 135 Pg dry matter (DM) yr-1 contributing to the 10% of the global annual emission of acetone and methanol (Matthews, 1997; Warneke et al., 1999). It

was found that the leaves litter contribution to acetone and methanol emissions is due to the degradation processes driven by microorganisms or abiotic factor (i.e., temperature), process known to release partially oxidized VOC such as acetone and methanol (Warneke et al., 1999).

45 The composition and amount of BVOCs emitted from leaves litter, alongside their associated reactivity, strongly depend on plant species, decomposition state, and environmental conditions such as temperature, ultraviolet (UV) light irradiation, and ozone concentration. Nevertheless, ozone concentration in rural areas has been estimated to be around 60 ppb, with peaks reaching 80 ppb during summer (Monks et al., 2015). This affect leaves litter directly through chlorosis and cellular damage (Diaz-de-Quijano et al., 2016). Although, ozone indirectly impacts biological and chemical processes such as photosynthesis,
50 respiration, stomatal functioning (Yendrek et al., 2017), and the emissions of BVOCs (Yuan et al., 2016, 2017). Another important factor affecting the degradation of leaves litter is UV light (Derendorp et al., 2011), which is responsible for increased emissions of short length VOCs (i.e., C2-C5) especially in the presence of humid air (Derendorp et al., 2011).

This study aims to investigate the individual and combined effects of ozone and UV light irradiation on BVOCs emission and
55 the subsequent SOA formation from rapeseed litter, Brassica Napus sp. The rapeseed litter was used since it is the third most cultivated species after wheat and maize in France (French National Statistics, 2019). We investigated the VOC emission profiles of the senescent rapeseed leaves for 6 days after they were collected. The experiments have been carried out in a multiphase simulation chamber during which, leaves litter were exposed to (i) UV light (UV), (ii) ozone (O_3), and (iii) a combination of both (UV_O_3).

2 Materials and Methods

2.1 Samples collection

The leaves of Rapeseed (sp. Brassica napus) used during the experiments were collected on June 3rd, 2019 in the AgroParisTech field, Thiverval-Grignon (48°85′N, 1°95′E). The Thiverval-Grignon site is located about 30 km west of Paris, North of France. The soil of this site is classified as Luvisol, which consists of 25% clay, 70% silt, and 5% sand. The site is
65 15 ha and the rapeseed leaves have been collected using the random sampling method. To avoid inhomogeneous samples in terms of the decomposition stage, all the leaves have been cut directly from the stems. The leaves samples have been stored for 2 days in a refrigerated chamber at 4°C until the measurement started.

2.2 Samples preparation

The rapeseed leaves have been acclimatized for about 2h hours at 20°C before being inserted in the multiphase simulation
70 chamber. In this way, leaves reached room temperature, which corresponds to the average temperature in the north of France during summertime. This was necessary for the reproduction of real-time conditions under which the rapeseed leaves start their decomposition. Once acclimatized, leaves have been weighted and spread on to cover the whole surface of a FEP (fluorinated ethylene propylene) film (with a surface of 0.64 m²) (**Figure 1a**). After 6 days of measurement, the surface covered by the rapeseed litter has been estimated to be 0.45 m² (**Figure 1b**) using Adobe Photoshop software (V 21.1.1). Photoshop
75 allowed the manual selection of the pixel containing the litter, the pixel has been converted in surface area (m²) using the following formula:

$$A_{litter} = \frac{Px_{litter}}{Px \times m^2} \qquad (\text{eq. 1})$$

where A_{litter} is the area covered by the rapeseed litter 6 days after the beginning of the experiment, Px_{litter} is the number of
80 pixel in the litter area, and $Px \times m^2$ is the number of pixels per m². The initial weight of rapeseed in the chamber ranged from 75 to 80 g. Meanwhile, after 6 days of measurement the weight decreased by 29-32 %. After being spread on the FEP, the samples were introduced into the multiphase simulation chamber.

2.3 Multiphase simulation chamber

The multiphase atmospheric simulation chamber is schematized in **Figure 2**. The atmospheric chamber has a rectangular shape
with 1m length $\times$ 1m width $\times$ 2m height (total volume 2 m³). The chamber is made of FEP film. The chamber has been
continuously filled with 6 L min⁻¹ of purified air, where 2 L min⁻¹ of this total flow have been directed inside a glass bubbler
to maintain a constant relative humidity inside the chamber (RH= 50±5 %) (**Figure 2**). The overall air renewal time in the
chamber was around 5h30, which allows for chemical reactions to occur. The chamber was equipped with 12 UV lamps
(OSRAM lamps, Eversun L80W/79- R), 6 on the left wall and 6 on the right wall of the chamber. The spectrum of the UV
lamps is reported in the supplementary information (**Fig. S1**). Temperature, relative humidity, and differential pressure (to
ensure a slight overpressure in the chamber compared to laboratory air) have been monitored using a combined sensor for
temperature and relative humidity (Vaisala HUMICAP humidity, and Temperature Probe HMP110; Vaisala Differential
Pressure Transmitter PDT101). VOCs and particle formations were monitored using a high-resolution proton transfer reaction
mass spectrometer (PTR-TOF-MS 8000, Ionicon Analytik) and a scanning mobility particle sizer spectrometer (SMPS - model
3080, TSI), respectively.

2.4 Experimental set-up

The rapeseed litter has been studied within a multiphase simulation chamber which allowed the closest representation of the
atmospheric conditions. The rapeseed litter has been tested under three different conditions to distinguish the potential factors
influencing the VOC emissions and the particle formation. The chosen conditions were under (i) UV light irradiation, (ii)
ozone, and (iii) ozone and UV light irradiation at the same time. The UV light irradiation has been turned off and on following
the night/day cycle; the UV light has been turned on for a total of seven hours per day. The ozone has been injected once a day
into the chamber, at the same time as the UV light was turned on, with a concentration of 80 ppb that was progressively
consumed during the day. Finally, every sample was analysed during 6 days for each of the previously mentioned conditions.

2.5 Particles measurement

Particles have been detected by means of a SMPS consisting of a differential mobility analyzer (DMA, model 3085, TSI) and
an ultrafine condensation particle counter (UCPC model 3776 high flow, TSI, d_{50}>2.5 nm). During the experiments, the
scanning particle size ranged from 2.5 to 79.1 nm, and both the sheath and sample flow rates were settled at 3 and 0.3 L min⁻¹,
respectively. The SMPS inlet was positioned at 180 cm, above the rapeseed surface, to observe the particle formation and
growth. The density of measured particles was assumed to be 1 g cm⁻³. The particles loss due to the impact of the chamber
walls has been calculated based on data from previous experiments performed on the same multiphase simulation chamber
(Alpert et al., 2017; Bernard et al., 2016). The estimation of the particles loss used for the correction of the SMPS data have
been resumed in the supplementary information, Fig. S2.

2.6 VOCs measurement

VOCs have been detected using the PTR-TOF-MS technique, which has been already described in detail by Müller et al.,
(2014). Ionization of the VOCs has been carried out using the H_3O^+ mode. The pressure and voltage of the drift tube have been
respectively set to 2.2 mbar and 500 V with a temperature of 80°C. Consequently, the E/N ration was about 123 Td (1 Td=10⁻¹⁷
V cm²). These parameters have been maintained constant during the whole experiment to avoid different ionization conditions
of the VOCs within the drift tube. The sample inlet of the PTR-TOF-MS has been constantly heated at 60°C to avoid product
loss by absorption in the inlet tube. The instrument sampled every 30 seconds with a flow rate of 100 mL/min; and the raw
data has been recorded using the TofDaq software (Tofwerk AG, Switzerland).

Moreover, the calibration of the spectra has been performed via both an oxygen isotope of the ion source $H_3^{18}O^+$ (21.022 m/z)
and an ionized acetone molecule $C_3H_7O^+$, (59.0449 m/z) as described by Cappellin et al. (Cappellin et al., 2011). Those

compounds have been chosen for the calibration because their identification was straightforward for all the samples kinds used in this study.

125 After calibrating the spectra, a peak table was created including the largest number of detected compounds. The threshold for the automatic research feature of the peak has been settled at 0.1 counts per second. Even if the peaks have been automatically identified, a manual readjustment of every peak has been performed to reduce the bias of the automatic peak research. The range of the detected masses was between 31 m/z and 164 m/z. Masses deriving from the water cluster such as 37.03 m/z, 38.03 m/z, 39.03 m/z, and 55.03 m/z were not taken into account during the analysis of the dataset.

130 Furthermore, the mixing ratio (ppb) has been calculated using the PTR-viewer software (V3.2.8, Ionicon, Analytik GmbH) which used the equation described in Cappellin et al., (2011); and the VOC emissions fluxes (E_{VOC}) in µg m^{-2} h^{-1} have been calculated as follow:

$$E_{VOC} = \frac{F_{air} \times ([VOC]_{litter} - [mVOC]_{blank}) \times M_{VOC}}{V_{mol}^{air} \times ((S_{litter-S} + S_{litter-E})/2) \times 1000 \ (ng/\mu g)} \qquad (eq.\ 2)$$

where F_{air} is the net airflow (F_{air} = 240 L h^{-1}), $[VOC]_{litter}$ is the concentration (ppb) of the VOC emitted in the chamber with

135 the samples, and $[VOC]_{blank}$ which is the concentration (ppb) of the VOC measured in the empty chamber. M_{VOC} is the molecular mass of the corresponding VOC (g mol^{-1}), V_{mol}^{air} is the air molar volume at standard temperature and pressure (24.79 L mol^{-1} at 25°C and 1 atm), and $S_{litter-S}$ is the exposed surface of litter to light when the experiment started and $S_{litter-E}$ is the exposed surface of litter to light when the experiment ended.

2.6.1 Peaks identification method

140 The spectra have been analyzed using the Spectra Analyser tool of the PTR viewer software (Version 3.2.8, Ionicon). This tool allowed the identification of the compounds corresponding to each peak among the spectra, by searching the possible combinations of elements leading to the closest molecular weight. This identification of the VOC has been also double-checked with literature reviews. Even if this method accounted for the most precise identification of the VOCs, it does not provide a certain identification of the compounds since, (1) it is not possible to distinguish between two ion masses that are closer than

145 the PTR-TOF-MS mass resolution, and (2) the PTR-TOF-MS does not distinguish between isomers (VOCs having the same molecular mass). The PTR-TOF-MS has a mass resolution of 4500 m/Δm.

2.6.2 Data analysis

The database was filled with 217 variables corresponding to the number of detected masses for the three different conditions UV, O$_3$, and UV_O$_3$ (as mentioned previously). The statistical analysis of the entire dataset has been performed using the R

150 software (Version 1.2.5019– ©2009–2019 RStudio). At first, we selected the variables that were normally distributed by the Shapiro-Wilk test (W>0.9). Secondly, we tested the homogeneity of the variance by the Levene-test to perform the Analysis of Variance (ANOVA) test followed by the Tukey post-hoc test. Furthermore, we tested the differences between the conditions using the Principal Component Analysis (PCA – package *FactormineR*). The PCA allowed a graphical representation of the whole dataset differentiating the VOCs emission profiles for the different tested conditions without bias. A table with the 30

155 most emitted compounds and their relative abundance at the three different conditions is presented in **Table 1**. The correlation between the VOC and particles formation has been calculated using the basic package STAT of R studio. The Spearman correlation was chosen as method since the distribution of the dataset was not normal. Finally, VOC compounds with a correlation level lower than -0.6 have been discussed.

3 Results

3.1 Ozone and UV light irradiation effect on the average VOC concentrations

VOC emissions have been measured for 6 days for each condition. The summed VOC emissions from the different conditions showed a statistical difference for every day of measurement. Under UV irradiation (the first condition), the summed VOC emissions kept increasing until the 5th day of measurement, while during the last day it statistically decreased (**Figure 3a**). Whereas, for the conditions O_3 and UV_O_3 (second and third conditions), the summed VOC emissions increased the 2nd day, and then slowly decreased from the third to the 6th day of measurement (**Figure 3b** and **3c**).

Furthermore, the ANOVA test confirmed a difference between the averages of the summed VOC emissions per day. These results highlight a statistical increase of the summed VOC emissions under UV irradiation (first condition) and a statistical decrease of the summed VOC emissions among time for the O_3 and the UV_O_3 condition. The summed VOC emissions were higher for the UV condition than for the UV_O_3 condition. The condition with the lowest VOC emission rate was with ozone.

The VOC emission profiles of the different conditions are compared in Figure 4. The PCA shows that the VOC profiles emitted during the UV condition were strongly different from the VOC profiles emitted from the UV_O_3 and O_3 conditions. Meanwhile the UV_O_3 and the O_3 modalities had very similar profiles since their ellipses are superposed (Figure 4). The major differences in the emission profiles were led by the different concentrations of 10 compounds at following m/z: 45.03, 45.99, 46.03, 47.02, 49.99, 59.049, 60.05, 73.03, 108.95 and 125.95. Those compounds are also among the 30 most emitted compounds trough all three conditions (Table 1). The identification of the 30 most emitted compounds for the three different conditions are listed in the supplementary information, Table S1.

The 30 most emitted compounds represented 90 % of the summed VOC emissions for each condition. The list of the most emitted compound between the O_3 condition and UV_O_3 condition was similar especially in terms of types of emitted compounds. The three most emitted compounds for these two conditions were methanol (CH_3OH^+, 33.03 m/z), acetaldehyde ($C_2H_4OH^+$, 45.03 m/z), and butyric acid ($C_4H_8O_2H^+$, 89.05 m/z) while for the UV condition the three most emitted VOC were acetic acid (61.03 m/z), acetone (59.049 m/z), and methanol (33.03 m/z). The average contribution of the VOCs over the 6 measurement days showed a large difference for each condition. For instance, methanol contributed to 9%, 32 %, and 50%, for UV, O_3, and UV_O_3, respectively.

3.2 Evolution and diversity of the VOC emissions per day

For the UV light experiments, small changes have been observed. For example, the average contribution of acetic acid (m/z 61.03) increased between 10-15 % during days 3 to 5 compared to days 1, 2, and 6, while that of methanol (33.03 m/z) increased by 5% during days 2 and 3. However, the other most emitted VOCs contribution was constant during that time (**Figure 5a**). For the O_3 condition, the most important variation in the average contribution is represented by the mass 33.03 m/z, which increased by 7% between the 4th and the 6th day (**Figure 5b**). It is also worth mentioning that masses 42.03 m/z and 49.99 m/z contributed to less than 0.01% of the total VOC emissions during the 1st and 2nd day of measurements, while after 3 days their contribution increased by 80 and 200 fold-change reaching 0.8% and 2% of the VOC relative abundance, respectively. The average contribution of the mass 89.06 m/z decreased over time from 5 % during the first day to 0.5% during the 6th day of measurements. Similar behavior was reported for the mass 73.06 m/z, where its average contribution increased to 8% during the 2nd and 3rd measurement day and then decreased to 0.5% of the average contribution during the 6th day. Analyzing the UV_O_3 condition, we noticed that the variation in the VOC contribution per day is higher than for the other conditions. In addition, results in **Figure 5c** reported that the mass 71.05 m/z was strongly emitted during the 6th day of measurement (30%), whereas this VOC emission did not reach 0.01 % of the contribution in the previous days. The average contribution of the mass 33.03 m/z decreased over time passing from 70% on the 1st and 2nd day till 30% on the 6th day of measurements.

Moreover, the Shannon Index, representing the diversity of emitted VOC, has been calculated for every day of measurements
200 to highlight an increase or a decrease of the VOC diversity with time. The VOC Shannon index showed that there is no
statistical differences in terms of VOC diversity that were observed for the UV light condition (S.I. 3.05 – 3.28) and O_3
condition (p.value >0.05). Concurrently, the UV_O_3 condition results showed a statistically significant increase of the VOC
diversity with time (from 1.54 to 2.4). The Shannon index of the VOC also showed a significantly larger Shanonn index for
the UV condition compared to the UV_O_3 condition (3.15 compared to 2). An intermediate value of 2.35 was obtained for the
205 O_3 condition.

3.3 Ozone and UV light irradiation effect on particle formation

Concurrently with the detection of VOC emissions, we also investigated particle formation for the three different conditions.
Under UV irradiation, nucleation started 1 hour after switching on the UV light (**Figure 6a**). The initial nucleation produced
a dense number of particles between 5×10^4 and 8×10^4 particles cm^{-3}. Then, the number of particles decreased, while their
210 diameter increased from 2 nm to 40 nm. Likewise, under ozone condition (**Figure 6b**), a nucleation event started also 1 h after
the injection of 80 ppb of ozone. However, compared to the UV light irradiation experiment, the ozone injection led to a lower
number of particles formed (2.5×10^4 particles cm^{-3}) with a smaller diameter (<17 nm). Nevertheless, when the UV light
irradiation was combined with ozone injection (third condition), the nucleation was stronger than the first two cases reaching
a maximum of 3.5×10^5 particles cm^{-3} for particles diameters between 2 and 12 nm (**Figure 6c**). Ozone depletion was also faster
215 than in the case where O_3 was only used (i.e. condition two).

Furthermore, **Figure 8** regroup the 10 VOC negatively correlated with the SOA formation for the UV_O_3 condition. The
negative correlation means that VOCs decreased alongside an increase of the SOA number concentration. Those compounds
have a Spearman coefficient lower than -0.60. For the other VOC not displayed in **Figure 8,** non-significant correlations were
found along the SOA formation.

220 **4 Discussion**

4.1 UV light and Ozone affect the diversity of the VOC emission profiles.

For the O_3 and UV_O_3 experiments, the VOC diversity decreased while the methanol contribution increased. Potard et al.,
(2017) observed similar behaviors in their experiment, which consisted of measuring VOC emissions from soils receiving
different types of amendment: the highest methanol average contribution corresponded to the lowest VOC diversity. Moreover,
225 differentiated VOC profiles have been highlighted in the PCA (**Figure 4**) between the UV light experiment and the O_3 and
UV_O_3 experiments. Several mechanisms are regulating the VOC emissions, and thus affecting the VOC diversity. These
mechanisms are discussed in the following paragraphs in detail.

4.2 Effect of ozone and UV light irradiation on the most emitted compounds

Methanol (CH_4OH^+, 33.03 m/z). Methanol was the most emitted compound in O_3 and UV_O_3 conditions. Methanol emission
230 from plants is ubiquitous (Bracho-Nunez et al., 2011; Gonzaga Gomez et al., 2019; Harley et al., 2007; Wiß et al., 2017a).
Moreover, methanol is the most emitted VOC from crops and other plants such as *Cistus albidus, Coronilla valentina, and*
Prunus persica (Harley et al., 2007), and it contributes often to more than half of the overall VOCs emissions. Hence, in our
study, the methanol average contribution to the total VOCs emission is between 8.9 % (under UV) and 50 % (under UV and
O_3). Gonzaga Gomez et al., (2019) measured VOC emissions from rapeseed using dynamic chambers and reported that
235 methanol contributed from 56 to 77% of the summed VOC emissions. These values are higher than in the current study. The
reason behind this difference could be that Gonzaga Gomez et al., (2019) measurements were performed over the whole
growing plant while in our experiment, we only analyzed the emission from leaves litter. Furthermore, the emissions of

methanol from leaves depend on the phenological stage of the plant (Wiß et al., 2017b), which could be another factor differentiating this study from that of Gonzaga Gomez et al., (2019). In fact, in this study, we measured mature leaves in the

240 last phenological state, while Gonzaga Gomez et al., (2019) analyzed leaving plants in the flowering and grain filling stages. Mature leaves are known for emitting less methanol than young ones (Harley et al., 2007). Methanol is produced via the demethylation of the pectin by the Pectin Methyl Esterase (PME) activity. This process occurs during the cell wall growth which is an intense process happening during the early stage of leaf expansion (Fall and Benson, 1996). Comparing the results obtained for the UV_O₃ condition with that of Harley et al., (2007), where their experimental conditions were the closest to

245 those used here, we found that the methanol emissions were in the same range. The emission flux of methanol under UV_O₃ condition in the current study is 0.22 ± 0.03 µg g^{-1} h^{-1}, while Harley et al., (2007) reported fluxes ranging from 0.2 to 2.7 µg g^{-1} h^{-1} for mature leaves. Moreover, under the UV condition, our results show a higher emission rate of methanol compared to the other conditions which are in line with previous studies that demonstrated how the UV light increased the methanol emissions from leaves (Derendorp et al., 2011; Harley et al., 2007).

250 **Acetaldehyde** (C$_2$H$_4$OH$^+$, 45.03 m/z). Acetaldehyde was the second most emitted compound for the O₃ condition and the 3rd and the 4th most emitted for the UV_O₃ and UV experiments, respectively. In general, the mechanisms leading to acetaldehyde emissions are still uncertain. The most accreditated hypothesis is that these emissions are correlated to different types of stress such as ozone exposure and leaf damage (chlorosis) caused by the sunlight (Seco et al., 2007). In this study, leaves were under high ozone concentration (60-80 ppb) and intense UV irradiation, which could have accelerated the senescence period of the

255 rapeseed leaves inside the chamber. As a result of these stressing conditions, we obtained larger acetaldehyde emissions than in previous studies. For instance, Greenberg et al., (2012) reported a VOC flux for leaves litter under the canopy of 0.3 µg m^{-2} h^{-1}, while in this study the emission flux ranged from 1.97 ± 0.01 µg m^{-2} h^{-1} for the UV_O₃ case to 26.7 ± 0.2 µg m^{-2} h^{-1} for the UV one. However, Hörtnagl et al., (2014) reported a burst of 1900 µg m^{-2} h^{-1} after a meadow cutting. Nonetheless, another pathway for the production of acetaldehyde is the ethanol oxidation at the leaf level forming acetaldehyde (Niinemets et al.,

260 2014; Seco et al., 2007). This process only occurs in anaerobic condition since it is the consequence of the ethanolic fermentation pathway. Hence, acetaldehyde can be formed in leaf tissues, but this pathway cannot be the main reason for the acetaldehyde emissions detected in this study, since the leaves litter was not in an anoxic environment. The magnitude of the acetaldehyde emission rate detected is similar to the one detected by Bachy et al., (2016) from soil hosting C4 crops (7 ± 9 µg m^{-2} $_{soil}$ h^{-1}). Therefore, we underline the possibility that rapeseed leaves litter might contribute to tropospheric acetaldehyde

265 emissions at the same level as soil and plants under environmental stress conditions.

Acetoin (C$_4$H$_8$O$_2$H$^+$, 89.06 m/z). Acetoin was the second and the third most emitted compound for the conditions UV_O₃ and O₃ respectively with an average contribution to the summed VOC emissions between 9 and 11%. This compound has been already reported as one of the most emitted compounds from bacteria dwelling in rapeseed samples (Wagner et al., 2018). These bacteria have been identified as *Enterobacter*, *Klebsiella*, *Serratia*, *Staphylococcus*, and *Streptomyces* (Schulz and

270 Dickschat, 2007). The pyruvate metabolic pathway of the microorganisms just listed allows the production of the acetoin molecule by the decarboxylation of acetolactate (Schulz and Dickschat, 2007). The large production of this compound can be attributed to the presence of bacteria colonizing the leaves surfaces and also to the favorable conditions for the bacteria growth such as optimal temperature (T= 25 °C) (Membre et al., 2005), and a humid atmosphere (RH= 50%) (Mceldowney and Fletcher, 2008) in our experiments.

275 **Acetone** (C$_3$H$_6$OH$^+$, 59.049 m/z). This compound was largely emitted from litter under UV light. The average contribution of acetone was 13% for the UV light condition and 1.64 and 2 % for the UV_O₃ and O₃ conditions, respectively. Acetone has been reported as one of the most emitted compounds by plants (Gonzaga gomez et al., 2019). For instance in the study of Gonzaga Gomez et al.,(2019), where the VOC detection has been performed at a different phenological stage of the rapeseed plant, acetone was detected among the most emitted VOCs from leaves and was correlated with sunlight, since the highest

280 emission peak of acetone occured at midday. These findings are in line with the higher emissions of acetone in the UV light

experiment but not with the UV_O₃ experiment. Furthermore, Cojocariu et al., (2005) found that under stress conditions such as high O₃ concentration, the acetone concentration increased in *Fagus selvatica* which is in contrast with the results of this study, where the O₃ concentration seems to reduce the acetone emissions. The biogenic nature of the source of acetone cannot be confirmed since, as reported by Das et al., (2003), acetone emissions could be the result of photochemical reactions of other
285   VOCs. Decaying and senescing plants may be another direct source of acetone (Warneke et al., 1999; Jacob et al., 2002; Karl et al., 2003).

4.2.1 Other emitted compound

Isoprene (C5H8H+, 69.07 m/z). In this study, isoprene was the 30th most emitted compounds only in the experiment without O₃. Its average contribution in the UV light experiment was 1% with a flux rate of 3.00 ± 0.03 µg m^{-2} h^{-1} or 0.02 µg g^{-1} h^{-1}
290   which is almost 20 times lower than the emissions reported by Morrison et al., (2016), where the maximum detected flux of isoprene from rapeseed was 0.35 µg g^{-1} h^{-1}. This difference is probably due to the branch emissions from Morrison et al., (2016), while in this study only the emissions from senescent leaves were considered. Furthermore, mature leaves are known to emit less isoprene than young leaves (Bracho-Nunez et al., 2011; Kuzma and Fall, 1993), which could explain the higher emission rate found in Morrison et al., (2016) study, where growing plants were analyzed. However, the flux rate of isoprene
295   reported by this study is in line with the reported flux rate of 0.035 µg g^{-1} h^{-1} by Gonzaga Gomez et al., (2019).

4.3 SOA formation from leaves litter BVOC emissions

Up to our knowledge, the investigation of the SOA formation from leaves litter samples has only been reported by the study of Faiola et al., (2014). Faiola et al., (2014) reported the maximum peak volume of the SOA particles obtained through the oxidation of the emitted VOCs by the injection of 130 ppb of O₃ under controlled atmospheric conditions. The experiment was
300   similar to the one performed here, where only 80 ppb of ozone were injected (O₃ condition). Comparing the O₃ experiment in this study with the experiment under dry conditions of Faiola et al., (2014) (**Table 2**), the maximum volume of SOA particles in our study has the same order of magnitude than the volume reported by Faiola et al., (2014). The most important difference between this study and the previous one is the concentration of the monoterpenes detected. In Faiola et al., (2014) monoterpenes contributed to 80% of the total VOC emissions. Monoterpenes, together with isoprene and sesquiterpenes, are
305   considered as the three primary classes of VOCs forming SOA (Sakulyanontvittaya et al., 2008). Isoprene is the most emitted compound from vegetation (Sindelarova et al., 2014) with a relatively small aerosol yield (Henze and Seinfeld, 2006). On the other hand, monoterpenes have been known to widely contribute to SOA formation (Griffin et al., 1999). In this study, monoterpenes were found to be lower than our PTR-TOF-MS detection limit, and isoprene was only the 30th most emitted compound under UV light irradiation. These findings led to the hypothesis that other mechanisms involving the VOCs
310   negatively correlated with the SOA formation, listed in **Figure 8**, are efficiently operating. For instance, furfural have been reported as a precursor of SOA formation with an aerosol yield ranging from 0.3 to 3% depending on the ozone concentration (Colmenar et al., 2020). Acetaldehyde and acetone have been reported to be uptaken into the aerosol phase and to participate to the aerosol-phase reactions (Barsanti and Pankow, 2004). Those reactions generate products with a relatively low vapor pressure, which leads to an additional partitioning from the gas phase increasing the organic particulate mass (Limbeck et al.,
315   2003; Tong et al., 2006). In this study, acetaldehyde and acetone have been found to be correlated with the SOA formation and to be largely emitted, from 60 to 40 and from 17 to 12 ppb respectively, in the UV_O₃ condition, from rapeseed leaves litter. The observed particles formation highlighted the high oxidation potential of the UV light irradiation with a volume of particle production per day higher than the one found for the O₃ experiment (**Table 2**). Moreover, the combination of the ozone and the UV light produced a larger maximum aerosol volume peak than the one reported in Faiola et al., (2014) for both, dry
320   and wet conditions and the largest aerosol volume per day compared to the O₃ and UV light experiments (**Table 2**).

Furthermore, we observed particles in the range from 2.5 to 79.1 nm, while Faiola et al., (2014) detected them between 20 and 730 nm. In this study, for the O_3 experiment, the percentage of particles under 20 nm contributed to 38% of the total aerosol volume (**Table 2**). Therefore, aerosol formation from leaves litter was certainly underestimated in this previous study due to the importance of particles below 20 nm.

325 **4.4 Atmospheric implications**

This study highlighted the possibility that emissions from rapeseed leaves litter, one of the three most cultivated crops in France and worldwide, have been underestimated. We reported a substantial SOA formation for the different studied conditions. Moreover, in the experiment with UV and O_3, the aerosol volume measured in the chamber was 790 μm^3 cm^{-3}. It is important to stress that these results may correspond to lower limits for SOA production since (i) the UV lamps had about

330 seven times lower light intensity at 365 nm than the actual solar radiation, (ii) the detection of the particles formation have been performed up to 79.1 nm, consequently, the formation of particles having greater diameters have not been detected. We, therefore, suggest that a SOA formation from leaves litter may have an atmospheric impact. This study also highlights the need for further studies to quantify the possible impact of the SOA formation from leaves litter at a larger scale.

4.4 Conclusions

335 In this work, we detected the VOC from rapeseed litter samples for 6 days under three different conditions: UV light irradiation, ozone injection, and UV light combined with ozone injection. The experiment was performed under controlled conditions within an atmospheric simulation chamber. The results showed that BVOC emissions from senescent rapeseed litter impact the SOA formation and that the combination of UV light irradiation and ozone injection increased the BVOC emission profiles diversity. The UV light irradiation was found to affect the production of the SOA more than the O_3 injection. In the presence

340 of both UV light and O_3 the SOA formation was 9 and 52 times higher than solely UV light or ozone, respectively.
Low emissions of isoprene were detected, even though, the production of SOA was not negligible. Other compounds, were found to be negatively correlated with the SOA formation, and thus to be possible precursors of the SOA formation from leaves litter. The densest portion of particles produced by litter samples had a diameter lower than 20 nm which might have caused the underestimation of the SOA formation from litter in other studies that detected a range of particles with a diameter

345 higher than 20 nm.

Acknowledgments
This work has received funding from the Agence de la transition écologique (ADEME) under the Cortea program (RAVISA grant agreement No. 1762C0006), and the European Commission (EC) under the European Union's Horizon 2020 research
350 and innovation program (Eurochamp 2020 grant agreement No. 730997).

Author contribution
Abis L., conceptualization, data curation, investigation, formal analysis, methodology, Visualization, writing – original draft preparation. **Kalalian** C. methodology, investigation, Writing – review & editing. **Lunardelli** B. methodology, investigation.
355 **Wang** T., data curation, investigation. **Perrier** S. investigation, methodology, resources. **Loubet** B, Writing – review & editing, investigation. **Ciuraru** R., conceptualization, data curation, methodology, Writing – review & editing, Funding acquisition, project administration, supervision, validation. **George** C., methodology, Writing – review & editing, Funding acquisition, project administration, supervision, validation.

360 **Competing interests**
The authors declare that they have no conflict of interest.

References

Alpert, P. A., Ciuraru, R., Rossignol, S., Passananti, M., Tinel, L., Perrier, S., Dupart, Y., Steimer, S. S., Ammann, M., Donaldson, D. J. and George, C.: Fatty Acid Surfactant Photochemistry Results in New Particle Formation, Sci. Rep., 7(1), 365 12693, https://doi.org/10.1038/s41598-017-12601-2, 2017.

Bachy, A., Aubinet, M., Schoon, N., Amelynck, C., Bodson, B., Moureaux, C. and Heinesch, B.: Are BVOC exchanges in agricultural ecosystems overestimated? Insights from fluxes measured in a maize field over a whole growing season, Atmospheric Chem. Phys., 16(8), 5343–5356, https://doi.org/10.5194/acp-16-5343-2016, 2016.

Barsanti, K. C. and Pankow, J. F.: Thermodynamics of the formation of atmospheric organic particulate matter by accretion 370 reactions—Part 1: aldehydes and ketones, Atmos. Environ., 38, 4371–4382, https://doi.org/10.1016/j.atmosenv.2004.03.035, 2004.

Bernard, F., Ciuraru, R., Boréave, A. and George, C.: Photosensitized Formation of Secondary Organic Aerosols above the Air/Water Interface, Environ. Sci. Technol., 50(16), 8678–8686, https://doi.org/10.1021/acs.est.6b03520, 2016.

Bigg, E. K.: Gas emissions from soil and leaf litter as a source of new particle formation, Atmospheric Res., 70(1), 33–42, 375 https://doi.org/10.1016/j.atmosres.2003.10.003, 2004.

Bracho-Nunez, A., Welter, S., Staudt, M. and Kesselmeier, J.: Plant-specific volatile organic compound emission rates from young and mature leaves of Mediterranean vegetation, J. Geophys. Res. Atmospheres, 116(D16), https://doi.org/10.1029/2010JD015521, 2011.

Cappellin, L., Biasioli, F., Granitto, P. M., Schuhfried, E., Soukoulis, C., Costa, F., Märk, T. D. and Gasperi, F.: On data 380 analysis in PTR-TOF-MS: From raw spectra to data mining, Sens. Actuators B Chem., 155(1), 183–190, https://doi.org/10.1016/j.snb.2010.11.044, 2011.

Cojocariu, C., Escher, P., Häberle, K.-H., Matyssek, R., Rennenberg, H. and Kreuzwieser, J.: The effect of ozone on the emission of carbonyls from leaves of adult Fagus sylvatica, Plant Cell Environ., 28(5), 603–611, https://doi.org/10.1111/j.1365-3040.2005.01305.x, 2005.

385 Colmenar, I., Martín, P., Cabañas, B., Salgado, S., Villanueva, F. and Ballesteros, B.: Evaluation of the SOA Formation in the Reaction of Furfural with Atmospheric Oxidants, Atmosphere, 11(9), 927, https://doi.org/10.3390/atmos11090927, 2020.

Das, M., Kang, D., Aneja, V. P., Lonneman, W., Cook, D. R. and Wesely, M. L.: Measurements of hydrocarbon air–surface exchange rates over maize, Atmos. Environ., 37(16), 2269–2277, https://doi.org/10.1016/S1352-2310(03)00076-1, 2003.

De Gouw, J. and Jimenez, J. L.: Organic Aerosols in the Earth's Atmosphere, Environ. Sci. Technol., 43(20), 7614–7618, 390 https://doi.org/10.1021/es9006004, 2009.

Derendorp, L., Holzinger, R. and Röckmann, T.: UV-induced emissions of C2–C5 hydrocarbons from leaf litter, Environ. Chem., 8(6), 602–611, https://doi.org/10.1071/EN11024, 2011.

Diaz-de-Quijano, M., Kefauver, S., Ogaya, R., Vollenweider, P., Ribas, À. and Peñuelas, J.: Visible ozone-like injury, defoliation, and mortality in two Pinus uncinata stands in the Catalan Pyrenees (NE Spain), Eur. J. For. Res., 135(4), 687–696, 395 https://doi.org/10.1007/s10342-016-0964-9, 2016.

Faiola, C. L., Vander Schelden, G. S., Wen, M., Elloy, F. C., Cobos, D. R., Watts, R. J., Jobson, B. T. and Van Reken, T. M.: SOA Formation Potential. of Emissions from Soil and Leaf Litter, Environ. Sci. Technol., 48(2), 938–946, https://doi.org/10.1021/es4040045, 2014.

Fall, R. and Benson, A. A.: Leaf methanol — the simplest natural product from plants, Trends Plant Sci., 1(9), 296–301, 400 https://doi.org/10.1016/S1360-1385(96)88175-0, 1996.

French National Statistics: https://agreste.agriculture.gouv.fr/, https://agreste.agriculture.gouv.fr/, 2019.

Gonzaga gomez, L., Loubet, B., Lafouge, F., Ciuraru, R., Buysse, P., Durand, B., Gueudet, J. C., Fanucci, O., Fortineau, A., Zurfluh, O., Decuq, C., Kammer, J., Duprix, P., Bsaibes, S., Truong, F., Gros, V. and Boissard, C.: Comparative study of biogenic volatile organic compounds fluxes by wheat, maize and rapeseed with dynamic chambers over a short period in 405 northern France, Atmos. Environ., 214, 16 p., https://doi.org/10.1016/j.atmosenv.2019.116855, 2019.

Granier, C., Pétron, G., Müller, J.-F. and Brasseur, G.: The impact of natural and anthropogenic hydrocarbons on the tropospheric budget of carbon monoxide, Atmos. Environ., 34(29), 5255–5270, https://doi.org/10.1016/S1352-2310(00)00299-5, 2000.

410 Greenberg, J. P., Asensio, D., Turnipseed, A., Guenther, A. B., Karl, T. and Gochis, D.: Contribution of leaf and needle litter to whole ecosystem BVOC fluxes, Atmos. Environ., 59, 302–311, https://doi.org/10.1016/j.atmosenv.2012.04.038, 2012.

Griffin, R. J., Cocker, D. R., Seinfeld, J. H. and Dabdub, D.: Estimate of global atmospheric organic aerosol from oxidation of biogenic hydrocarbons, Geophys. Res. Lett., 26(17), 2721–2724, https://doi.org/10.1029/1999GL900476, 1999.

Guenther, A.: A global model of natural volatile organic compound emissions, J. Geophys. Res., 100(D5), 8873–8892, https://doi.org/10.1029/94JD02950, 1995.

415 Hallquist, M., Wenger, J. C., Baltensperger, U., Rudich, Y., Simpson, D., Claeys, M., Dommen, J., Donahue, N. M., George, C., Goldstein, A. H., Hamilton, J. F., Herrmann, H., Hoffmann, T., Iinuma, Y., Jang, M., Jenkin, M. E., Jimenez, J. L., Kiendler-Scharr, A., Maenhaut, W., McFiggans, G., Mentel, T. F., Monod, A., Prévôt, A. S. H., Seinfeld, J. H., Surratt, J. D., Szmigielski, R. and Wildt, J.: The formation, properties and impact of secondary organic aerosol: current and emerging issues, Atmospheric Chem. Phys., 9(14), 5155–5236, https://doi.org/10.5194/acp-9-5155-2009, 2009.

420 Harley, P., Niinemets, Ü. and Guenther, A.: Environmental controls over methanol emission from leaves, Biogeosciences Discuss., 4, https://doi.org/10.5194/bgd-4-2593-2007, 2007.

Hatfield, M. L. and Huff Hartz, K. E.: Secondary organic aerosol from biogenic volatile organic compound mixtures, Atmos. Environ., 45(13), 2211–2219, https://doi.org/10.1016/j.atmosenv.2011.01.065, 2011.

Henze, D. K. and Seinfeld, J. H.: Global secondary organic aerosol from isoprene oxidation, Geophys. Res. Lett., 33(9), 425 https://doi.org/10.1029/2006GL025976, 2006.

Hörtnagl, L., Bamberger, I., Graus, M., Ruuskanen, T. M., Schnitzhofer, R., Walser, M., Unterberger, A., Hansel, A. and Wohlfahrt, G.: Acetaldehyde exchange above a managed temperate mountain grassland, Atmospheric Chem. Phys., 14(11), 5369–5391, https://doi.org/10.5194/acp-14-5369-2014, 2014.

Isidorov, V. and Jdanova, M.: Volatile organic compounds from leaves litter, Chemosphere, 48(9), 975–979, 430 https://doi.org/10.1016/S0045-6535(02)00074-7, 2002.

Viros J, C, F., H, W., J, G., C, L. and E, O.: Litter of mediterranean species as a source of volatile organic compounds, Atmos. Environ., 242, 117815, https://doi.org/10.1016/j.atmosenv.2020.117815, 2020.

Jacob, D. J., Field, B. D., Jin, E. M., Bey, I., Li, Q., Logan, J. A., Yantosca, R. M. and Singh, H. B.: Atmospheric budget of acetone, J. Geophys. Res. Atmospheres, 107(D10), ACH 5-1-ACH 5-17, https://doi.org/10.1029/2001JD000694, 2002.

435 Karl, T., Guenther, A., Spirig, C., Hansel, A. and Fall, R.: Seasonal variation of biogenic VOC emissions above a mixed hardwood forest in northern Michigan, Geophys. Res. Lett., 30(23), https://doi.org/10.1029/2003GL018432, 2003.

Kesselmeier, J. and Staudt, M.: Biogenic Volatile Organic Compounds (VOC): An Overview on Emission, Physiology and Ecology, J. Atmospheric Chem., 33(1), 23–88, https://doi.org/10.1023/A:1006127516791, 1999.

Kuzma, J. and Fall, R.: Leaf Isoprene Emission Rate Is Dependent on Leaf Development and the Level of Isoprene Synthase, 440 Plant Physiol., 101(2), 435–440, https://doi.org/10.1104/pp.101.2.435, 1993.

Limbeck, A., Kulmala, M. and Puxbaum, H.: Secondary organic aerosol formation in the atmosphere via heterogeneous reaction of gaseous isoprene on acidic particles, Geophys. Res. Lett., 30(19), https://doi.org/10.1029/2003GL017738, 2003.

Matthews, E.: Global litter production, pools, and turnover times: Estimates from measurement data and regression models, J. Geophys. Res. Atmospheres, 102(D15), 18771–18800, https://doi.org/10.1029/97JD02956, 1997.

445 Mceldowney, S. and Fletcher, M.: The effect of temperature and relative humidity on the survival of bacteria attached to dry solid surfaces, Lett. Appl. Microbiol., 7, 83–86, https://doi.org/10.1111/j.1472-765X.1988.tb01258.x, 2008.

Membre, J., Leporq, B., Vialette, M., Mettler, E., Perrier, L., Thuault, D. and Zwietering, M.: Temperature effect on bacterial growth rate: quantitative microbiology approach including cardinal values and variability estimates to perform growth simulations on/in food, Int. J. Food Microbiol., 100(1–3), 179–186, https://doi.org/10.1016/j.ijfoodmicro.2004.10.015, 2005.

450   Monks, P. S., Archibald, A. T., Colette, A., Cooper, O., Coyle, M., Derwent, R., Fowler, D., Granier, C., Law, K. S., Mills, G. E., Stevenson, D. S., Tarasova, O., Thouret, V., von Schneidemesser, E., Sommariva, R., Wild, O. and Williams, M. L.: Tropospheric ozone and its precursors from the urban to the global scale from air quality to short-lived climate forcer, Atmospheric Chem. Phys., 15(15), 8889–8973, https://doi.org/10.5194/acp-15-8889-2015, 2015.

Morrison, E. C., Drewer, J. and Heal, M. R.: A comparison of isoprene and monoterpene emission rates from the perennial
455   bioenergy crops short-rotation coppice willow and Miscanthus and the annual arable crops wheat and oilseed rape, GCB Bioenergy, 8(1), 211–225, https://doi.org/10.1111/gcbb.12257, 2016.

Müller, M., Mikoviny, T., Feil, S., Haidacher, S., Hanel, G., Hartungen, E., Jordan, A., Märk, L., Mutschlechner, P., Schottkowsky, R., Sulzer, P., Crawford, J. H. and Wisthaler, A.: A compact PTR-ToF-MS instrument for airborne measurements of volatile organic compounds at high spatiotemporal resolution, Atmospheric Meas. Tech., 7(11), 3763–3772,
460   https://doi.org/10.5194/amt-7-3763-2014, 2014.

Murphy, J. G., Oram, D. E. and Reeves, C. E.: Measurements of volatile organic compounds over West Africa, Atmospheric Chem. Phys., 10(12), 5281–5294, https://doi.org/10.5194/acp-10-5281-2010, 2010.

Niinemets, Ü., Fares, S., Harley, P. and Jardine, K. J.: Bidirectional exchange of biogenic volatiles with vegetation: emission sources, reactions, breakdown and deposition, Plant Cell Environ., 37(8), 1790–1809, https://doi.org/10.1111/pce.12322, 2014.

465   Pfister, G., Emmons, L., Hess, P., Lamarque, J.-F., Orlando, J., Walters, S., Guenther, A., Palmer, P. and Lawrence, P.: Contribution of isoprene to chemical budgets: a model tracer study with the NCAR CTM MOZART-4, J. Geophys. Res., 113, https://doi.org/10.1029/2007JD008948, 2008.

Poisson, N., Kanakidou, M. and Crutzen, P. J.: Impact of Non-Methane Hydrocarbons on Tropospheric Chemistry and the Oxidizing Power of the Global Troposphere: 3-Dimensional Modelling Results, J. Atmospheric Chem., 36(2), 157–230,
470   https://doi.org/10.1023/A:1006300616544, 2000.

Potard, K., Monard, C., Le Garrec, J.-L., Caudal, J.-P., Le Bris, N. and Binet, F.: Organic amendment practices as possible drivers of biogenic Volatile Organic Compounds emitted by soils in agrosystems, Agric. Ecosyst. Environ., 250, 25–36, https://doi.org/10.1016/j.agee.2017.09.007, 2017.

Sakulyanontvittaya, T., Guenther, A., Helmig, D., Milford, J. and Wiedinmyer, C.: Secondary Organic Aerosol from
475   Sesquiterpene and Monoterpene Emissions in the United States, Environ. Sci. Technol., 42(23), 8784–8790, https://doi.org/10.1021/es800817r, 2008.

Schulz, S. and Dickschat, J. S.: Bacterial volatiles: the smell of small organisms, Nat. Prod. Rep., 24(4), 814–842, https://doi.org/10.1039/B507392H, 2007.

Seco, R., Penuelas, J. and Filella, I.: Short-chain oxygenated VOCs: Emission and uptake by plants and atmospheric sources,
480   sinks, and concentrations, Atmos. Environ., 41, 2477–2499, https://doi.org/10.1016/j.atmosenv.2006.11.029, 2007.

Sindelarova, K., Granier, C., Bouarar, I., Guenther, A., Tilmes, S., Stavrakou, T., Müller, J.-F., Kuhn, U., Stefani, P. and Knorr, W.: Global data set of biogenic VOC emissions calculated by the MEGAN model over the last 30 years, Atmospheric Chem. Phys., 14(17), 9317–9341, https://doi.org/10.5194/acp-14-9317-2014, 2014.

Tong, C., Blanco, M., Goddard, W. A. and Seinfeld, J. H.: Secondary Organic Aerosol Formation by Heterogeneous Reactions
485   of Aldehydes and Ketones: A Quantum Mechanical Study, Environ. Sci. Technol., 40(7), 2333–2338, https://doi.org/10.1021/es0519785, 2006.

Wagner, C., Bonte, A., Brühl, L., Niehaus, K., Bednarz, H. and Matthäus, B.: Micro-organisms growing on rapeseed during storage affect the profile of volatile compounds of virgin rapeseed oil, J. Sci. Food Agric., 98(6), 2147–2155, https://doi.org/10.1002/jsfa.8699, 2018.

490   warneke, C., Karl, T., Judmaier, H., Hansel, A., Jordan, A., Lindinger, W. and Crutzen, P.: Acetone, methanol, and other partially oxidized volatile organic emissions from dead plant matter by abiological processes: Significance for atmospheric HO(X) chemistry, Glob. Biogeochem. Cycles V13 9-15 1999, 13, https://doi.org/10.1029/98GB02428, 1999.

Wiß, F., Ghirardo, A., Schnitzler, J.-P., Nendel, C., Augustin, J., Hoffmann, M. and Grote, R.: Net ecosystem fluxes and composition of biogenic volatile organic compounds over a maize field–interaction of meteorology and phenological stages,
495   GCB Bioenergy, 9(11), 1627–1643, https://doi.org/10.1111/gcbb.12454, 2017a.

Wiß, F., Ghirardo, A., Schnitzler, J.-P., Nendel, C., Augustin, J., Hoffmann, M. and Grote, R.: Net ecosystem fluxes and composition of biogenic volatile organic compounds over a maize field–interaction of meteorology and phenological stages, GCB Bioenergy, 9(11), 1627–1643, https://doi.org/10.1111/gcbb.12454, 2017b.

500 Yendrek, C. R., Erice, G., Montes, C. M., Tomaz, T., Sorgini, C. A., Brown, P. J., McIntyre, L. M., Leakey, A. D. B. and Ainsworth, E. A.: Elevated ozone reduces photosynthetic carbon gain by accelerating leaf senescence of inbred and hybrid maize in a genotype-specific manner, Plant Cell Environ., 40(12), 3088–3100, https://doi.org/10.1111/pce.13075, 2017.

Yuan, X., Calatayud, V., Gao, F., Fares, S., Paoletti, E., Tian, Y. and Feng, Z.: Interaction of drought and ozone exposure on isoprene emission from extensively cultivated poplar, Plant Cell Environ., 39(10), 2276–2287, https://doi.org/10.1111/pce.12798, 2016.

505 Yuan, X., Feng, Z., Liu, S., Shang, B., Li, P., Xu, Y. and Paoletti, E.: Concentration- and flux-based dose–responses of isoprene emission from poplar leaves and plants exposed to an ozone concentration gradient, Plant Cell Environ., 40(9), 1960–1971, https://doi.org/10.1111/pce.13007, 2017.

Ziemann, P. J. and Atkinson, R.: Kinetics, products, and mechanisms of secondary organic aerosol formation, Chem. Soc. Rev., 41(19), 6582–6605, https://doi.org/10.1039/C2CS35122F, 2012.

510
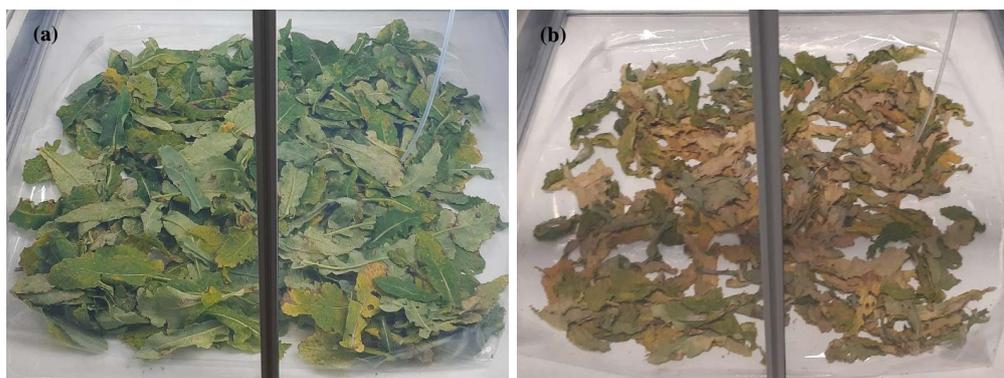
Figure 1: Example of the Rapeseed litter condition a) during the first day of the VOC and particles measurements and b) after 6 days of VOC and particles measurements.

515
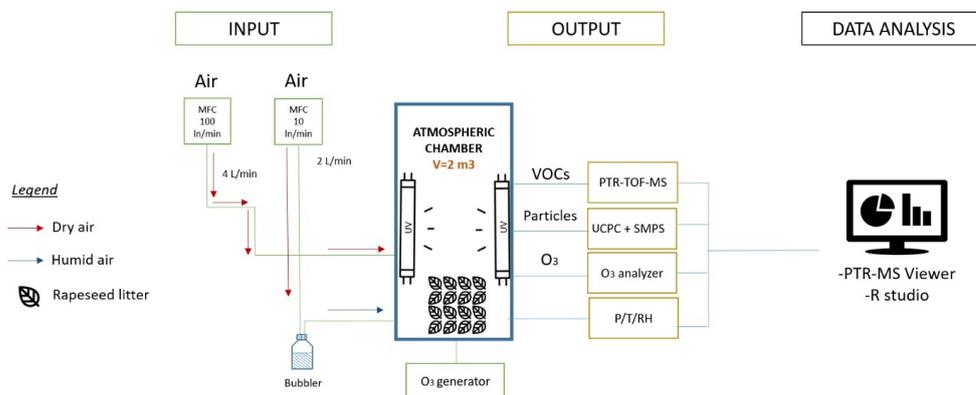
Figure 2: Scheme of the multiphase reaction chamber used for the study of the photoreactivity of the VOCs emitted from senescence rapeseed. The PTR-TOF-MS have been used for the VOCs detection, the ultrafine condensation particle counter (UCPC) and the SMPS have been used for the detection of the particle formation and measure the size particles, the O$_3$ analyzer detected the ozone
520 **inside the chamber, where P= pressure, T=temperature, and RH=relative humidity has been constantly monitored during the entire experiment.**
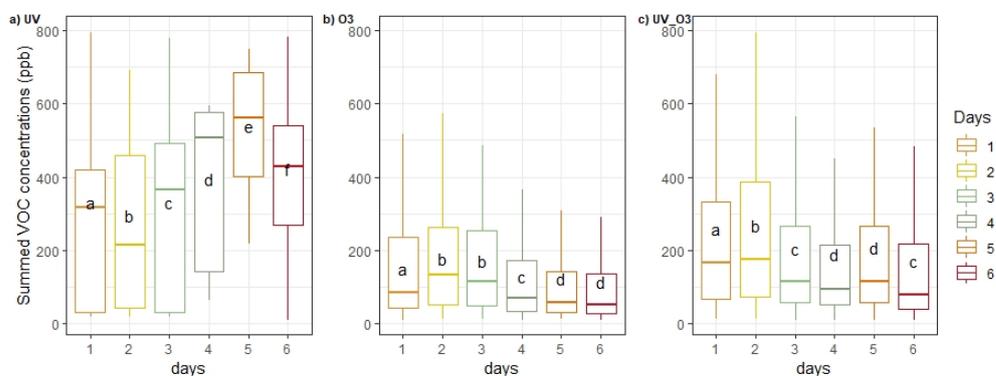
Figure 3: Summed VOC concentrations for each incubation condition a) UV, b) O3 and c) UV_O3 Letters indicate the statistical difference obtained by the Tukey test.
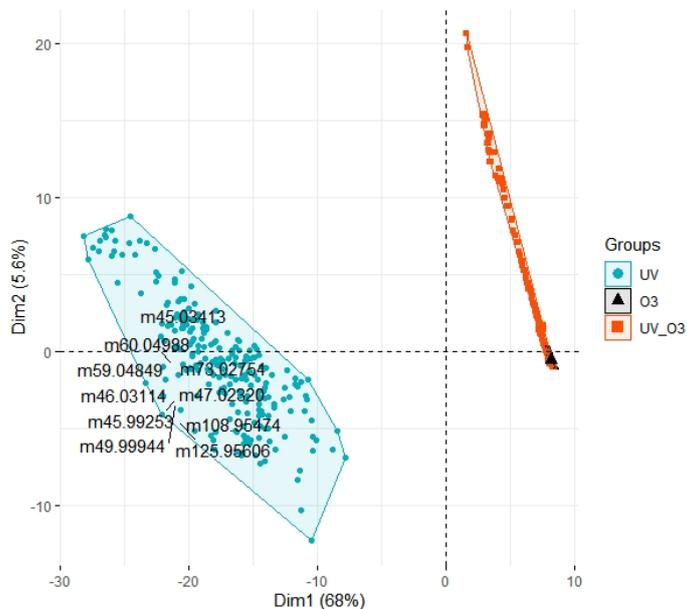
525

Figure 4: VOC profiles differences between UV light, UV_O₃, and O₃ conditions. The percentage of the variance explained by the 2 first components is shown on each axis (Dim1 and Dim2).
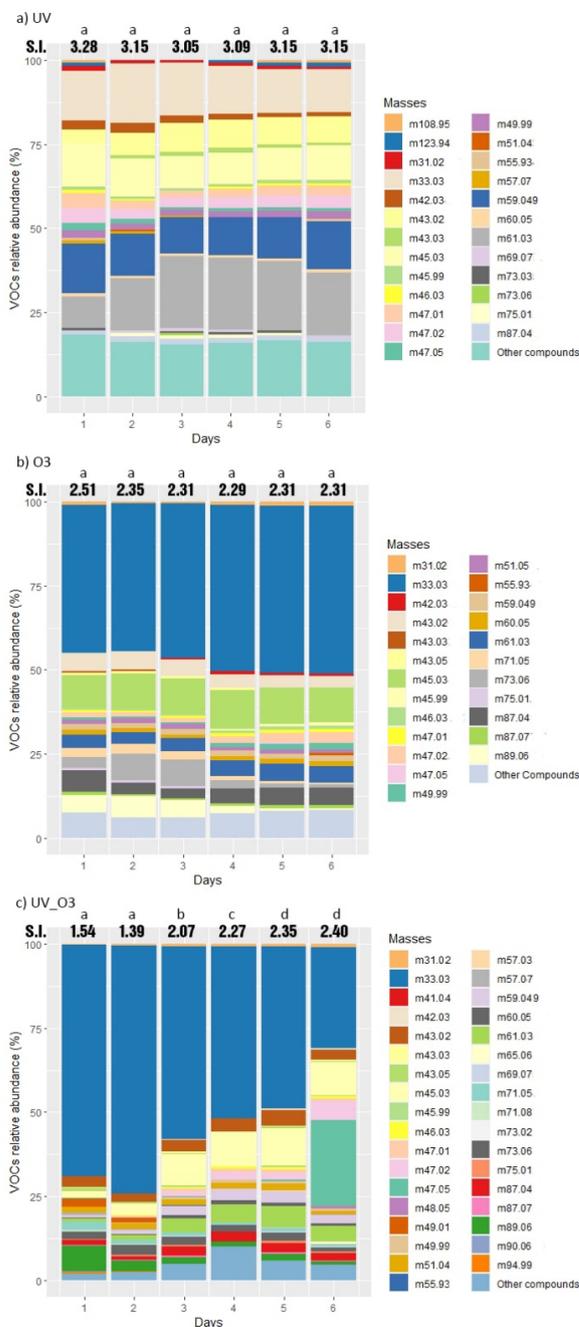
Figure 5: VOC relative abundance for rapeseed litter samples under a) UV light b) O₃ and c) UV_O₃ conditions. S.I. is the Shannon index representing the diversity of the VOC (for each day). Letters indicate significant differences of the S.I. according to the Tukey test with p.value < 0.05.
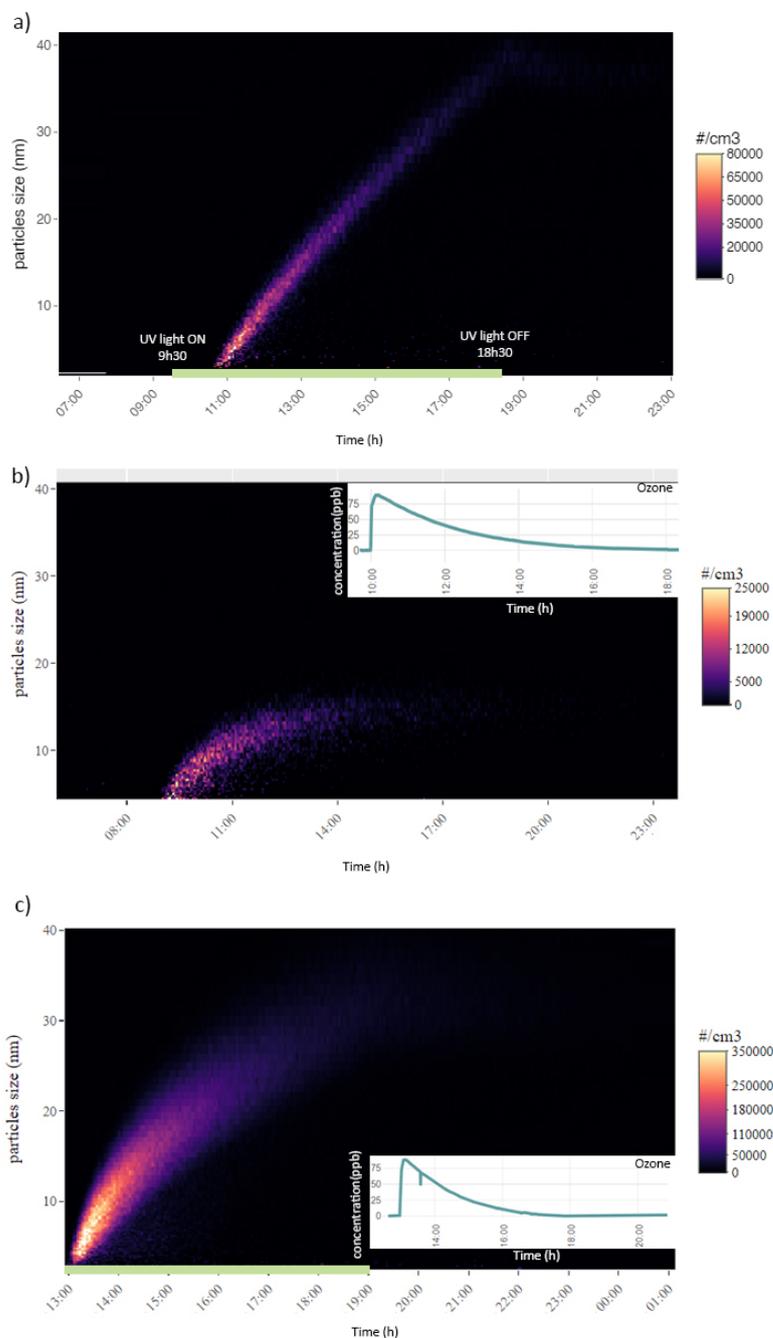
Figure 6. Temporal evolution of particle number and size distribution, ordinate represents the electrical mobility diameter (nm) and the colour scale the particle number concentration. Particle formation for the first day of measurement under a) UV light irradiation, b) Ozone injection and c) UV light irradiation and ozone injection combined. The green horizontal line represents the timeline where the UV light were switched on, for a) the UV light have been turned on at 9h30 and turned off at 18h30, for c) the UV light have been turned on at 12h30 and turned off at 19h. b) and c) also display the Ozone concentration timeline during the particle formation.

535
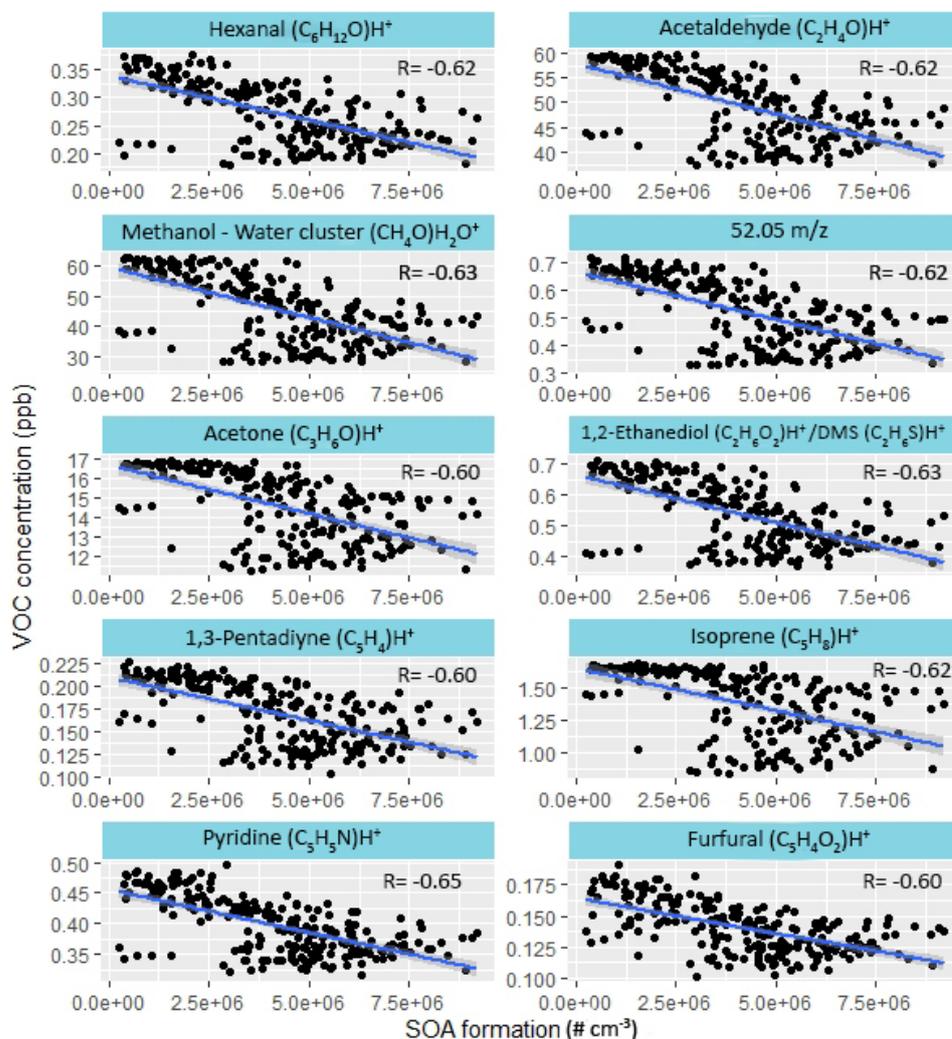
Figure 7 Correlation between VOC mixing ratios and total particles number observed under the UV_O₃ condition. The 10 most
540 correlated VOC are shown. The Pearson correlation coefficients (R) are also displayed for all correlations.

Table 1. The average of 30 most emitted compound during the 6 days of measurement for the three different modalities: UV light
irradiation, Ozone, and UV light irradiation and ozone at the same time. Within the columns m/z, the compounds highlighted as the
most differentiating between the VOC profiles by the PCA are in bold. A tentative identification of the compound here listed is
545 reported in Table S1.

MOST CONCENTRATED COMPOUNDS (UV)			MOST CONCENTRATED COMPOUNDS (O₃)			MOST CONCENTRATED COMPOUNDS (UV_O₃)		
m/z	BVOC Flux (µg/m²/h) ± sd	Average contribution (%)	m/z	BVOC Flux (µg/m²/h) ± sd	Average contribution (%)	m/z	BVOC Flux (µg/m²/h) ± sd	Average contribution (%)
61.03	64.28±0.60	20.16	33.03	4.59±0.01	31.52	33.03	24.35±0.09	50.40
59.049	41.50±0.06	13.01	**45.03**	1.44±0.01	9.89	89.06	5.24±0.001	10.85
33.03	28.38±0.17	8.90	89.06	1.16±0.001	7.96	**45.03**	1.97±0.01	4.09
45.03	26.71±0.20	8.38	73.06	1.15±0.001	7.92	73.06	1.93±0.00	3.99

43.02	18.35±1.90	5.76	87.04	1.10±0.08	7.58	87.04	1.53±0.42	3.18
47.02	9.12±1.20	2.86	61.03	0.76±0.01	5.21	71.04	1.48±0.76	3.07
87.04	7.78±1.17	2.44	43.02	0.61±0.04	4.21	43.02	1.46±0.22	3.02
47.01	7.23±1.66	2.27	71.05	0.46±0.03	3.16	61.03	1.26±0.02	2.60
123.94	5.41±0.08	1.70	**59.049**	0.30±0.001	2.07	51.04	1.02±0.001	2.12
49.99	5.34±0.02	1.68	**47.02**	0.23±0.02	1.60	49.01	0.92±0.001	1.90
42.03	5.18±0.47	1.63	60.04	0.22±0.01	1.50	**59.049**	0.79±0.001	1.64
108.95	3.75±0.10	1.18	51.04	0.19±0.001	1.32	47.05	0.65±0.06	1.34
75.01	3.69±0.05	1.16	87.07	0.18±0.02	1.23	94.99	0.39±0.16	0.81
47.05	3.13±0.08	0.98	**49.99**	0.14±0.001	0.95	**47.02**	0.35±19.23	0.73
69.07	3.00±0.03	0.94	75.01	0.14±0.001	0.94	57.07	0.35±0.001	0.73
60.05	2.83±0.30	0.89	**47.01**	0.09±0.03	0.64	71.08	0.34±0.001	0.71
73.03	2.79±1.04	0.87	43.05	0.09±0.01	0.61	43.05	0.33±0.02	0.67
43.03	2.59±0.34	0.81	**46.03**	0.09±0.03	0.60	87.07	0.28±0.07	0.58
101.06	2.59±0.41	0.81	42.03	0.07±0.001	0.49	**60.05**	0.27±0.01	0.56
87.07	2.30±0.20	0.72	31.01	0.07±2.22	0.47	75.012	0.26±0.001	0.55
45.99	2.30±0.33	0.72	**45.99**	0.07±0.02	0.45	90.06	0.15±0.001	0.32
73.06	2.27±0.04	0.71	43.03	0.06±0.06	0.43	**47.01**	0.15±0.65	0.31
125.95	2.25±0.07	0.71	123.94	0.06±0.001	0.42	31.02	0.14±0.46	0.30
90.95	2.16±0.06	0.68	47.05	0.05±0.001	0.35	**49.99**	0.13±0.001	0.27
57.06	2.12±0.08	0.67	88.04	0.05±0.01	0.34	43.03	0.12±0.60	0.25
55.93	1.85±0.06	0.58	**73.03**	0.05±1.26	0.34	46.03	0.11±0.05	0.23
46.03	1.84±2.19	0.58	55.93	0.05±0.001	0.32	123.94	0.09±0.001	0.18
57.03	1.78±0.74	0.56	90.06	0.05±0.01	0.31	42.03	0.08±0.04	0.16
31.01	1.70±0.21	0.53	74.06	0.05±0.11	0.31	74.06	0.07±0.53	0.15
93.95	1.64±0.10	0.51	**108.95**	0.04±0.001	0.28	96.007	0.07±0.001	0.14

Table 2. Comparison of the SOA formation from leaves litter samples reported in this study and the literature.

Sample type	Sampling period	Measured particles range (nm)	Type of chamber	Experimental conditions	Maximum peak of aerosol formation (μm^3 cm^{-3})	Total Aerosol volume concentration (μm^3 cm^{-3})	Volume Contribution of particles < 20 nm	Ref.
Mix of: Pinus ponderosa, Pseudotsuga menziesii Pinus monticola, Larix	May-June 2012	20-730	atmospheric chamber (7.7 m^3)	130 ppb of O_3 in dry conditions	0.97-5.43	-	-	(Faiola et al., 2014)

occidentalis litter and soil								
Mix of: Pinus ponderosa, Pseudotsuga menziesii Pinus monticola, Larix occidentalis litter and soil	May-June 2012	20-730	atmospheric chamber (7.7 m³)	Reproducing raining event 130 ppb of O₃	0.29-2.55	-	-	(Faiola et al., 2014)
Brassica napus litter	June 2019	2.5-79.1	Multiphase simulation chamber (2m³)	60-80 ppb of O₃	0.2	15.1	38%	This study
Brassica napus litter	June 2019	2.5-79.1	Multiphase simulation chamber (2m³)	Only UV light	0.8	85.4	24%	This study
Brassica napus litter	June 2019	2.5-79.1	Multiphase simulation chamber (2m³)	60-80 ppb of O₃ and UV light	7.6	787.8	24%	This study